

The use of remote sensing indices derived from Sentinel 2 satellite images for the defoliation damage assessment of *Lymantria dispar*

Andrei Buzatu^{1,2}, Constantin Nețoiu¹, Bogdan Apostol^{1✉}, Ovidiu Badea^{1,2}

Buzatu A., Nețoiu C., Apostol B., Badea O., 2023. The use of remote sensing indices derived from Sentinel 2 satellite images for the defoliation damage assessment of *Lymantria dispar*. Ann. For. Res. 66(1): 123-138.

Abstract: Monitoring and assessing the phytosanitary status of forests is a crucial activity in forest protection field, and the use of satellite remote sensing has become increasingly prevalent in this regard. Satellite images offer valuable information in terms of time and space, particularly through the analysis of vegetation and biophysical indices. Within this context, the aim of the study was to explore the potential of satellite remote sensing methods to monitor and assess the extent of tree defoliation caused by the gypsy moth (*Lymantria dispar*). The research study was focused on a forest situated in the Oltenia region of Romania, which experienced a gradation period for the defoliator *L. dispar* between 2018 and 2020. To determine the extent of defoliation caused by *L. dispar* in 2020 and 2021, a rectangular network consisting of 70 one-hectare sample areas was implemented. Each sample area had a square shape with a side of 100 m. In each corner of the sample areas, sub-sample circles with a radius of 12.62 meters were established, in which visual observations regarding the defoliation levels were conducted. The study involved a comparison between thematic maps derived from ground observations and those based on specific remote sensing indices derived through the processing of Sentinel 2 satellite images, of the Ciuturica forest area during the years 2020 and 2021. The research study indicated that the canopy water content (CWC) index was the most suitable for assessing defoliation caused by *L. dispar*. Furthermore, the study highlighted that remote sensing methods could be very effective and easily applicable, complementing the field ground-based efforts in monitoring and assessing the impact of *L. dispar* infestations.

Keywords: defoliation assessment, forest protection, Sentinel 2 images, remote sensing indices, thematic map

Addresses: ¹"Marin Drăcea" National Institute for Research and Development in Forestry (INCDS), Voluntari, Ilfov, Romania. | ²Faculty of Silviculture and Forest Engineering, "Transilvania" University of Brașov, Romania.

✉ **Corresponding Author:** Bogdan Apostol (bogdanap_ro@yahoo.com).

Manuscript: received June 09, 2023; revised June 26, 2023; accepted June 27, 2023.

Introduction

Over time, forest ecosystems can be subject to the detrimental effects of both biotic and abiotic factors, which disrupt their development and compromise their functional roles. In this context, the monitoring and assessment of the phytosanitary status of forests play a vital role in forest protection. Notably, satellite remote sensing and its applications are becoming increasingly valuable in this regard, providing valuable tools for monitoring, and assessing forest health. The tree crown serves as an important element in the assessment of forest health, as it allows for the estimation of two key variables: foliage discoloration and defoliation. These parameters are closely linked to stress factors and are considered reliable indicators for assessing forest damage (Innes 1993, Arhrib et al. 2023). In many forest ecosystems, insect defoliation has been the major cause of disturbance leading to important timber and carbon losses (Fraser & Latifovic 2005). Defoliators are in many occasions the main factor responsible for the annual losses in forest yield (Fleming & Volney 1995), and frequently increase susceptibility to secondary host infection, driving direct changes in stand dynamics (Wulder & Franklin 2006).

Vegetation and biophysical indices derived from satellite images offer critical insights into forest health by providing valuable information in both temporal and spatial dimensions. The rapid advancements in technology and data processing techniques derived from remote sensing have significantly contributed to the growing interest among researchers to apply these methods in the field of forest protection. These factors are essential in establishing a robust forest ecosystem surveillance system based on satellite remote sensing techniques, laying a solid foundation for its development and implementation. Hence, the application of these methods enables the mapping and understanding of the spatial and temporal distribution patterns concerning the severity of damages caused by diverse biotic or abiotic

factors (Hall et al. 2016). To map vegetation or insect attacks, classification algorithms (both unsupervised and supervised) are employed to generate thematic maps. These maps provide valuable insights into the spatial distribution and extent of vegetation or insect-related disturbances. More recently, non-parametric classification techniques, such as regression tree classification, have gained prominence in the field (Marx & Kleinschmit 2017, Chávez et al. 2019). These methods have demonstrated comparable or even superior accuracy compared to traditional supervised or unsupervised classification approaches (Vorovencii 2015, Volke & Abarca-del-Rio 2020). The use of satellite images in forest protection activities has been a subject of study since the 1970s, coinciding with the advent of the first satellite programs such as Landsat 1 (1972) and SPOT 1 (1986). These pioneering efforts primarily took place in the United States of America and Canada, where significant research was conducted in this field. Thus, since 1974, the mapping of damage caused by the defoliator *Lambdina fiscellaria* (Guenée, 1857) was conducted using satellite images captured by Landsat sensors (Beaubien & Jobin 1974, Hall et al. 2016, Sturtevant et al. 2023). The availability of satellite images with a wide range of spatial resolutions has opened possibilities for implementing multi-scale approaches in remote sensing forestry applications. These approaches are particularly valuable for detecting and discriminating various objects within complex natural scenes, such as the dynamic processes of forest disturbances (Marceau & Hay 1999, Crocker et al. 2023). Moreover, the spectral signatures of satellite image bands offer valuable information for detecting, identifying, and classifying various forms of tree damage caused by biotic or abiotic factors (El Ahmadi et al. 2023). These spectral signatures capture the unique reflectance patterns exhibited by healthy and damaged vegetation, enabling the differentiation of specific types of damage

(Ciesla et al. 2008, Rullan-Silva et al. 2013). Until now in Romania, the monitoring of biotic stress factors has primarily relied on ground-based observations and direct assessments (Norma 6/2000, OG454/2003).

Within this context, the aim of the study was to explore the potential of satellite remote sensing methods to monitor and assess the extent of tree defoliation caused by the gypsy moth (*Lymantria dispar* Linnaeus, 1758). The main objective of this study was to conduct a comparative analysis between field evaluations and the specific indices derived from Sentinel satellite images in order to monitor and assess the defoliation caused by *L. dispar* in oak stands.

Materials and Methods

The research study was centered on a forest situated in the Oltenia region of Romania, which experienced a gradation period for the defoliator *L. dispar* between 2018 and 2020 (Figure 1). The Ciuturica forest (44° 15'N – 23° 31'E) is located within the administrative boundaries of Craiova Forest District. Covering an area of approximately 310 hectares, this forest predominantly comprises Turkey oak (*Quercus cerris*) and Hungarian oak (*Quercus frainetto*)

tree species, with an average age of 65 years.

Surveillance plays a crucial role in the integrated control of harmful agents, as it enables the assessment of their temporal evolution, spread patterns, and the resulting damage. The selection of appropriate surveillance methods depends on various factors, including the size of the forested area, the specific biotic or abiotic agents being monitored, and the tree species that are susceptible to these agents (Berryman 1986).

To determine the extent of defoliation caused by *L. dispar* in 2020 and 2021, a rectangular network consisted of 70 one-hectare sample areas was established. Each sample area had a square shape with a side of 100 meters. In each corner of these sample areas, sub-sample circles with a radius of 12.62 meters were established, in which visual observations regarding the defoliation levels were conducted (Figure 2).

In the climate and vegetation conditions of Romania, the gypsy moth exhibits significant population growth, particularly in oak forests found in the plains and hills. Additionally, selected poplar and willow plantations are also susceptible to infestation. The defoliation caused by the gypsy moth follows a distinct pattern

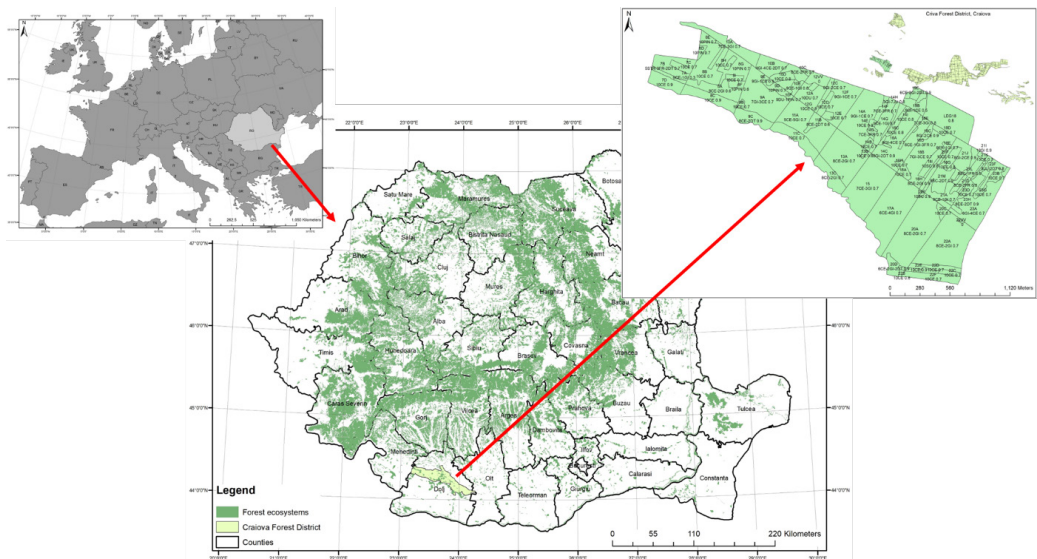


Figure 1 Study area located in southern part of Romania, in the Ciuturica forest, Craiova Forest District.

characterized by eruptive pulsations, with a cyclical occurrence approximately every 7 to 10 years. The specific duration of these cycles depends on the phytoclimatic characteristics and the structural composition of the forest stands.

The defoliation produced by the *L. dispar* was estimated by visual assessment of the crowns of the component trees of the circular sub-sample areas. This was expressed in integer percent values of five percent class (i.e., 5, 10, 15, 25, ..., 95, 100%), using as a reference a tree of the same species, with full foliage (Badea 2008, Badea et al. 2013).

The recorded data, represented in percentage

values, were categorized into five distinct levels of defoliation: very slight (1-10%), slight (11-25%), moderate (26-50%), severe (51-75%) and very severe (>75%) (Figure 3).

The data collected within the sub-sample circular areas, encompassing population density and the extent of defoliation caused by *L. dispar*, were used to generate thematic maps. Specific procedures such as the Inverse Distance Weighted function, implemented through the ArcGIS software, were employed to determine the areas affected by various levels of damage in the Ciuturica forest for the years 2020 and 2021. These maps offer valuable insights into the

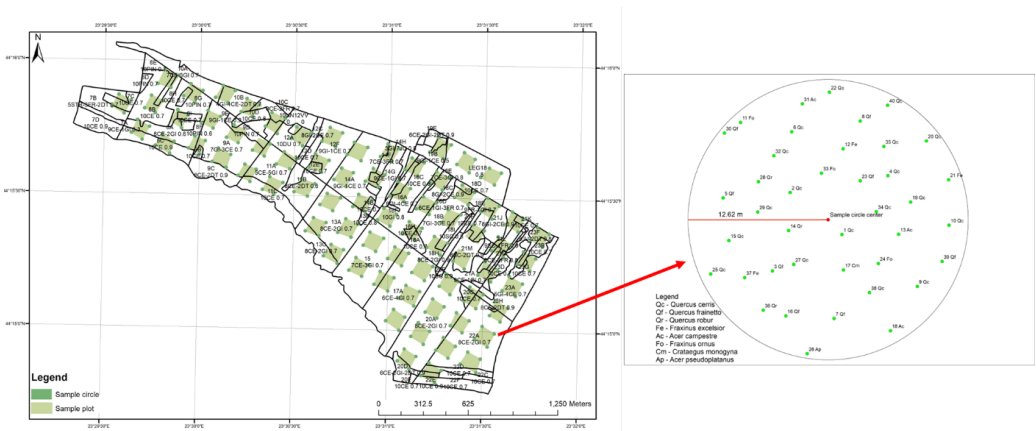


Figure 2 The rectangular network of sample areas located in the Ciuturica forest (Craiova Forest District) and the sub-sample circles where observations on defoliation were made.

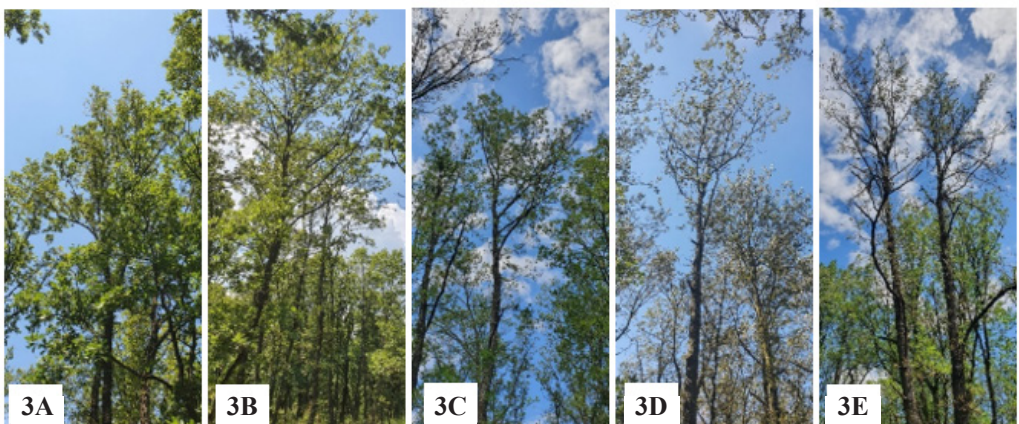


Figure 3 The intensity of tree damage classified by different levels of defoliation, made by *L. dispar* larvae (A – very slight, B – slight, C – moderate, D – severe, E – very severe).

spatial distribution and severity of the damage caused by *L. dispar* within this forest.

Given that the gypsy moth inflicts foliage damage, specific remote sensing techniques were employed to facilitate the surveillance, detection, and monitoring of their activity, as well as the assessment of defoliation level. These methods harness the power of satellite imagery and their specific processing techniques, enabling the effective assessment of the extent of damage caused by this defoliator.

To facilitate a comprehensive comparison between thematic maps derived from ground observations and those generated through specific processing of satellite images, Sentinel 2 satellite images were acquired for the Ciuturica forest area for the years 2020 and 2021 (Figure 4). These images were obtained to ensure a reliable and

accurate assessment of the forest's condition during the specified time period. The images were acquired using the Earth Explorer geoport (https://earthexplorer.usgs.gov/), an advanced application developed by the United States Geological Survey (USGS). The Earth Explorer geoport provides a wide range of satellite imagery from various missions, including the Sentinel 2 satellites. Due to the distinct spectral signature of vegetation in the near-infrared spectrum, satellite imagery has proven valuable in delineating various levels of tree damage (e.g., different levels of tree defoliation) (Gupta & Pandey 2021). To achieve this, the acquired images underwent specific processing procedures to derive remote sensing indices (Table 1). Existing literature suggests that vegetation indices are primarily derived from empirical evidence rather than

Table 1 Vegetation indices calculated based on Sentinel 2 Imagery.

Vegetation indices	Formula	Literature reference
Normalized Difference Vegetation Index (NDVI)	$NDVI = (NIR - R) / (NIR + R)$	(Rouse et al. 1974, Tucker 1979)
Difference Vegetation Index (DVI)	$DVI = NIR - R$	(Richardson & Wiegand 1977)
Perpendicular Vegetation Index (PVI)	$PVI = (NIR - a * R - b) /$	(Richardson & Wiegand 1977, Tucker 1979, Vorovencii 2015)
Normalised Difference Red Edge (NDRE)	$NDRE = (NIR - Re_{705}) / (NIR + Re_{705})$	(Barnes et al. 2000, Clarke et al. 2001, Hunt et al. 2011)
Vogelmann Red Edge Index (VREI)	$VREI = NIR / Re_{705}$	(Vogelmann et al. 1993)

Note: R – red band; NIR – Near Infrared band; a – slope of the soil line; b – gradient of the soil line; Re_{705} = Band 5 of Sentinel 2 (Vegetation Red Edge).

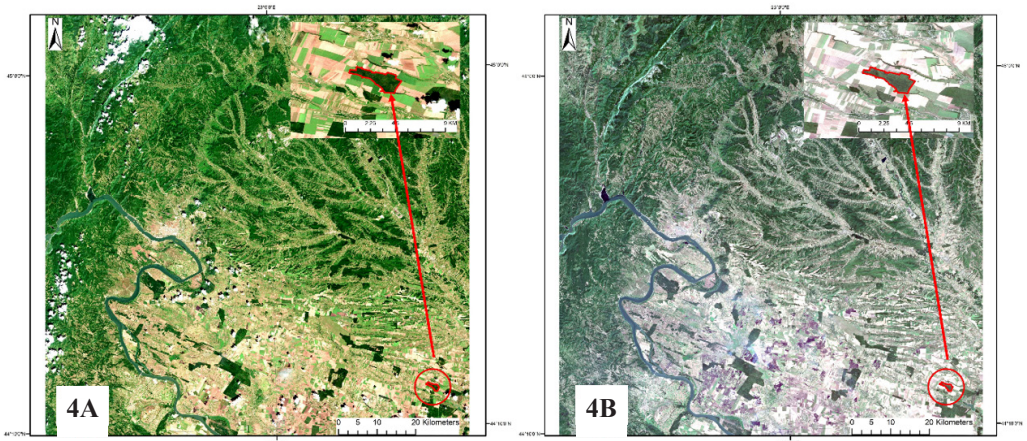


Figure 4 Full extend of Sentinel 2 satellite images (natural color coded) for 22.07.2020 (A) and 27.07.2021(B) highlighting the Ciuturica forest (the limit with red color).

being solely based on biological, physical, or chemical principles (Vorovencii 2015, Xue & Su 2017). Besides the vegetation indices, the biophysical ones are derived using algorithms that primarily involve generating databases containing vegetation characteristics and spectral reflectance data from the upper part of tree canopies. These databases are created by analyzing various satellite images, including Sentinel-2, Landsat 8, MERIS, and SPOT (Ali et al. 2020, Weiss et al. 2020).

Vegetation indices were determined using *Raster Calculator function* (*ArcGIS* software) (NDRE, VREI) or obtained using *SNAP* application (ESA Sentinel Application Platform v8.0) (NDVI, DVI, PVI). Furthermore, using the *SNAP* application, a biophysical index - Canopy Water Content (CWC) was calculated. This index provides an estimation of the water content stored in the leaves, measured per unit of surface area. The CWC index, derived through advanced processing techniques, offers valuable information about the moisture content within the vegetation canopy, which is crucial for assessing the health and vigor of the forest ecosystem (Cernicharo et al. 2013). It has been proved that there is a strong relationship between the reflectance of a vegetation canopy and its water content. Optical remote sensing techniques allow for the estimation of canopy water content by leveraging the water absorption features present in the spectral bands centered around 970 nm, 1,200 nm, 1,450 nm, and 1,950 nm (Curran 1989).

To analyze the data, the mean values of the pixels for each remote sensing derived indices were calculated using *Zonal Statistics as Table* (*ArcGIS* software), for each one-hectare sample area. Using the average level of defoliation assessed in the field and the corresponding average pixel values for each sample area, specific statistical methods such as linear regression and analysis of variance were employed to establish mathematical relationships between the defoliation values. This analysis was performed using the *Statistica*

12.0 software, considering both the observed field values and the pixel values derived from the remote sensing indices. Through image processing and the calculation of vegetation indices, it became possible to determine specific ranges of pixel values corresponding to different levels of defoliation. The ranges of pixel value variations obtained from the analysis were utilized to generate thematic maps representing the level of defoliation. The thematic maps derived from pixel values were then compared to the thematic maps obtained using field estimated defoliations.

Results

Since 2018, the defoliator *L. dispar* has experienced a population increase in the southern region of Oltenia Plain, leading to widespread infestation in various forest areas, including the Ciuturica forest, located within the administrative border of Craiova Forest District.

In the 2019-2020 generation, the defoliator population was in the phase of numerical growth, with densities that exceeded the critical level, on average, by 1.7 times (170% predicted defoliation). As a result of the uniformity of the infestations in space, achieved by the action of the wind in the young larva stage and natural mortalities, the defoliation achieved was far below the forecast, with an average of 23.4% and variations between 6% and 49%.

During the 2020-2021 generation, the population of the defoliator *L. dispar* transitioned from the numerical growth phase to the eruption phase, reaching densities that surpassed critical thresholds by an average of 2.9 times (equivalent to 290% predicted defoliation). However, in the spring of 2021, due to the substantial and widespread infestations within the forest area, aerial treatments in the form of aerial spray were implemented. As a result, the observed defoliation averaged at 12.4%, with variations ranging from 1% to 22%.

Using the field observations on the level of

defoliation caused by *L. dispar*, thematic maps were created to depict their spatial distribution based on different levels of intensity. These maps specifically represented the defoliation patterns for both the 2019-2020 and 2020-2021 generations (Figure 5). In 2021, there was a notable decrease in the intensity of defoliation compared to 2020 in the sampled areas. This decrease can be attributed to the specific pest control treatments that were implemented in the spring of 2021 to combat the infestation.

Based on the Sentinel 2 satellite images, a range of vegetation indices were derived using mathematical operations on various spectral bands. These indices exploit the vegetation's distinct characteristics, such as maximum absorption in the red and blue bands and high reflectance in the near infrared band. Additionally, the analysis involved the

calculation of biophysical indices like the Canopy Water Content (CWC), which provides valuable information about the water stored in the leaves on a per-unit surface basis.

The specific remote sensing indices, including NDVI, DVI, PVI, NDRE, VREI and CWC were obtained through a combination of software tools. The ESA Snap program played a significant role in calculating some of these indices (NDVI, DVI, PVI, and CWC). Additionally, the *ArcGIS* software was utilized to compute NDRE and VREI. These indices were specifically derived for the Ciuturica forest, considering the phenological moment after the gypsy moth had ceased feeding and disappeared (typically in the last decade of July) during the 2019-2020 and 2020-2021 generations (Figure 6).

In addition, a regression analysis was

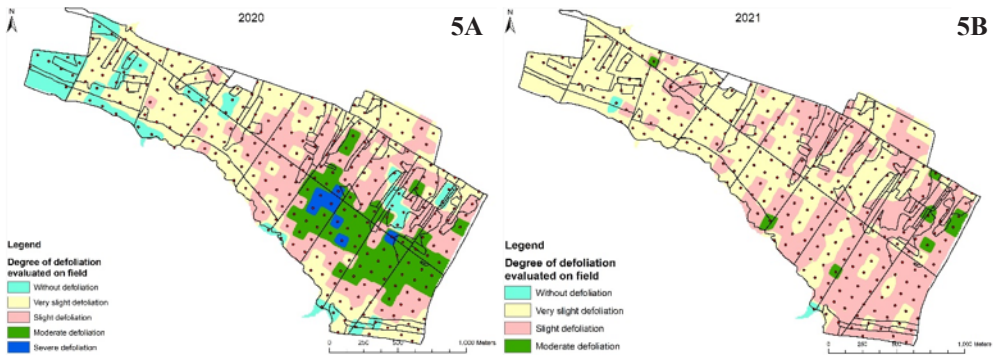
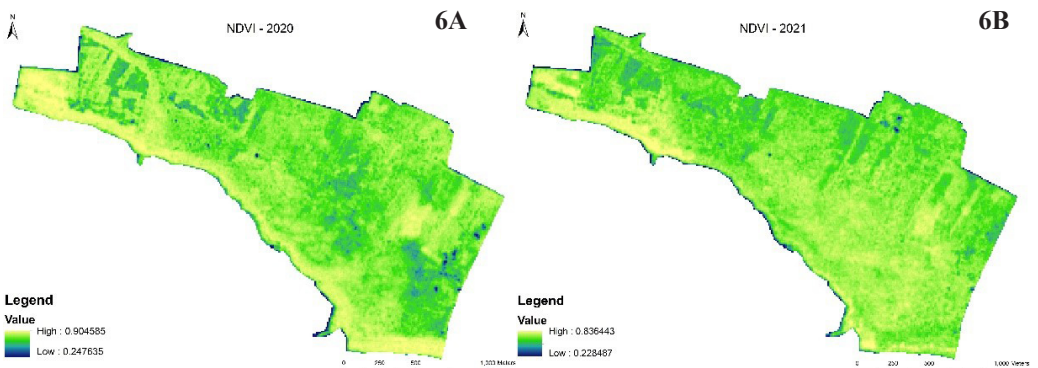
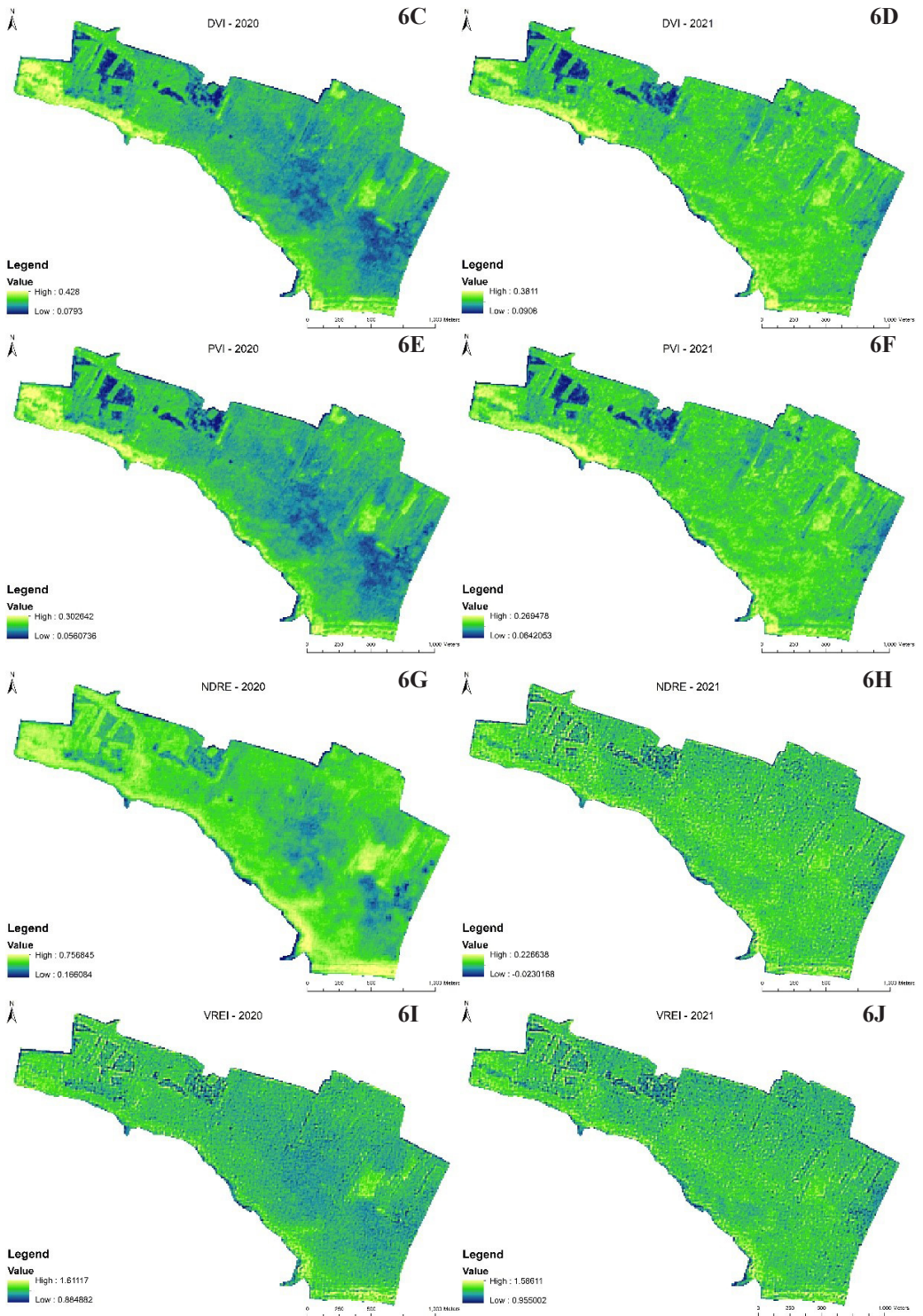


Figure 5 Thematic maps with the spatial distribution of defoliation by level of intensity made by *L. dispar*, the 2019-2020 generation (A) and the 2020-2021 generation (B), for the Ciuturica forest.





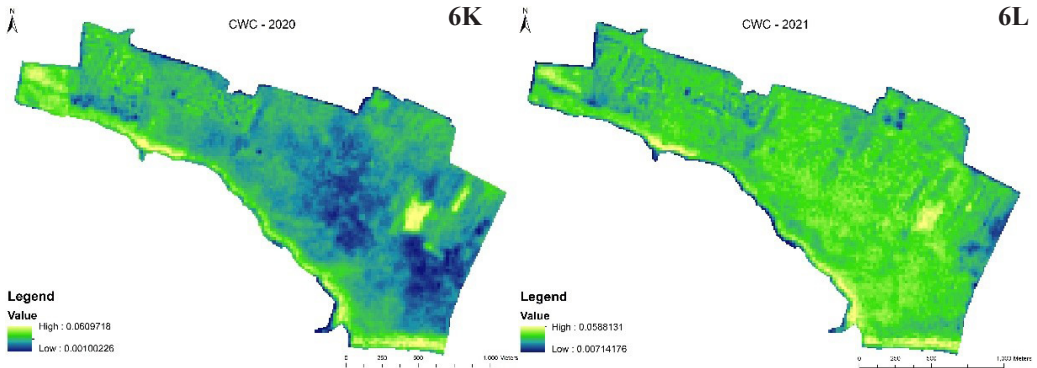


Figure 6 Indices calculated based on Sentinel 2 images for the Ciuturica forest – 22.07.2020 (NDVI - A), DVI – C), PVI – E) NDRE – G), VREI – I), CWC- K) and 27.07.2021 (NDVI - B), DVI – D), PVI – F) NDRE – H), VREI – J), CWC- L).

conducted to examine the correlation between defoliation levels, assessed in the field for each sampled surface, and the average pixel values corresponding to each vegetation index. This analysis was performed separately for the two vegetation seasons (2020 and 2021). The results revealed significant correlation coefficients for both years, ranging from 0.53 to 0.74 for the year 2020, and from 0.48 to 0.62, for 2021 (Table 2).

By conducting a simple analysis of variance, the standard errors, and the range of variation

relative to the mean of the pixel values were calculated for each derived remote sensing index. These calculations were performed for different levels of defoliation observed during the two consecutive years (2020-2021) (Table 3).

Analysis of the range of pixel value data in the two defoliation years reveals interesting findings regarding the NDVI and NDRE vegetation indices. It is observed that these indices exhibit varying degrees of overlap between different levels of defoliation, specifically between very slight and slight,

slight and moderate, and even between very slight and moderate defoliation levels. When analyzing the vegetation indices DVI, PVI, and VREI, it is evident that the ranges of pixel value variation in the two years are distinct. Specifically, there are small overlaps observed (0.002 for DVI and PVI, and 0.006 for VREI) between the very slight and slight levels of defoliation.

This observation indicates a higher level of stability in these indices when assessing the defoliation caused by

Table 2 Statistical parameters of specified indices calculated based on Sentinel 2 images and the correlation between pixel values and defoliation made by *L. dispar* (field assessment) for 2020 and 2021.

Derived index	\bar{X}	$\bar{X}-\sigma_X$ (min)	$\bar{X}+\sigma_X$ (max)	σ	r	Regression equation
2020						
DVI	0.272	0.240	0.288	0.025	-0.613**	Def. (%) = 97.227-299.5*DVI
VREI	1.228	1.194	1.249	0.026	-0.687**	Def. (%) = 400.64-313.5*VREI
NDRE	0.598	0.550	0.622	0.037	-0.602**	Def. (%) = 132.68-195.6*NDRE
NDVI	0.821	0.789	0.835	0.026	-0.538**	Def. (%) = 222.26-251.5*NDVI
PVI	0.192	0.170	0.203	0.017	-0.594**	Def. (%) = 96.311-419.5*PVI
CWC	0.033	0.026	0.038	0.005	-0.748**	Def. (%) = 71.086-1657*CWC
2021						
DVI	0.267	0.257	0.278	0.016	-0.516**	Def. (%) = 44.004-124.3*DVI
VREI	1.251	1.242	1.261	0.018	-0.495**	Def. (%) = 142.04-104.9*VREI
NDRE	0.111	0.108	0.115	0.007	-0.489**	Def. (%) = 39.491-257.9*NDRE
NDVI	0.738	0.724	0.753	0.024	-0.553**	Def. (%) = 76.285-88.71*NDVI
PVI	0.189	0.182	0.196	0.011	-0.516**	Def. (%) = 44.005-175.8*PVI
CWC	0.037	0.035	0.039	0.003	-0.620**	Def. (%) = 40.945-817.5*CWC

Note: \bar{X} - mean; σ_X - standard error; σ - standard deviation; r - correlation coefficient; * - level of significance, $p < 0.001$; Def(%) – field estimated defoliation

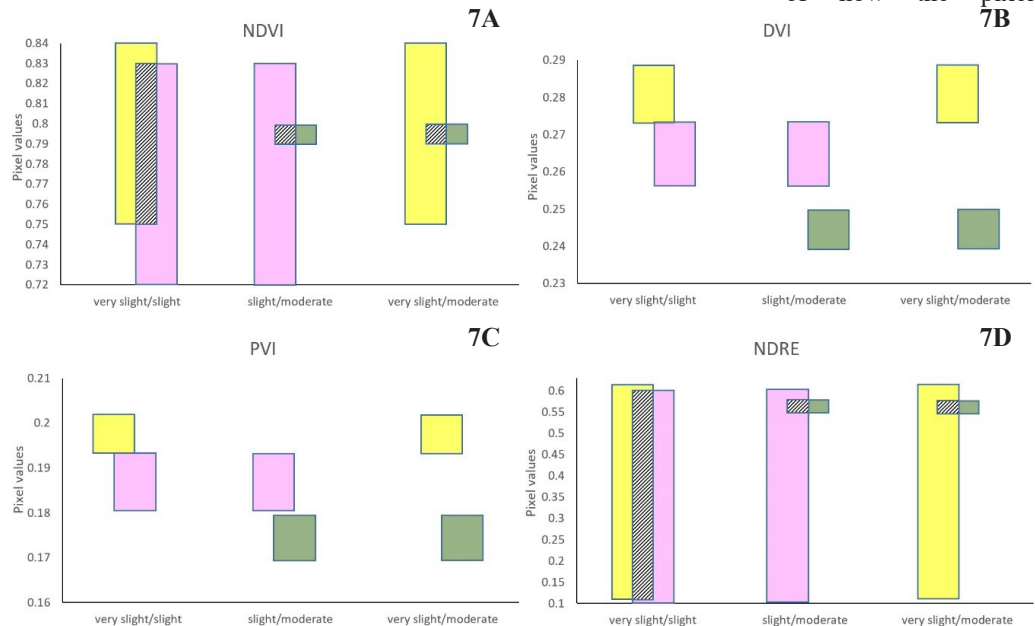
Table 3 Range of pixel value variation of the specified indices calculated based on the Sentinel 2 images.

Defoliation level	2020				2021				Pixel variation range 2020-2021* ($\bar{X}-\sigma_{\bar{x}}$; $\bar{X}+\sigma_{\bar{x}}$)
	\bar{X}	$\sigma_{\bar{x}}$	$\bar{X}-\sigma_{\bar{x}}$ (min)	$\bar{X}+\sigma_{\bar{x}}$ (max)	\bar{X}	$\sigma_{\bar{x}}$	$\bar{X}-\sigma_{\bar{x}}$ (min)	$\bar{X}+\sigma_{\bar{x}}$ (max)	
NDVI									
very slight	0.831	0.004	0.827	0.835	0.750	0.004	0.746	0.753	0.746-0.835
slight	0.824	0.005	0.819	0.828	0.727	0.004	0.724	0.731	0.724-0.828
moderate	0.795	0.006	0.789	0.801					0.789-0.801
DVI									
very slight	0.285	0.004	0.281	0.288	0.275	0.002	0.273	0.278	0.273-0.288
slight	0.271	0.004	0.267	0.275	0.259	0.002	0.257	0.262	0.257-0.275
moderate	0.245	0.005	0.240	0.250					0.240-0.250
PVI									
very slight	0.201	0.002	0.198	0.203	0.195	0.002	0.193	0.196	0.193-0.203
slight	0.192	0.003	0.189	0.195	0.183	0.002	0.182	0.185	0.182-0.195
moderate	0.174	0.004	0.170	0.177					0.170-0.177
NDRE									
very slight	0.616	0.005	0.611	0.622	0.114	0.001	0.113	0.115	0.113-0.622
slight	0.598	0.006	0.592	0.604	0.107	0.001	0.108	0.110	0.108-0.604
moderate	0.558	0.008	0.550	0.566					0.550-0.566
VREI									
very slight	1.245	0.003	1.242	1.249	1.258	0.003	1.255	1.261	1.242-1.261
slight	1.221	0.004	1.217	1.225	1.245	0.003	1.242	1.248	1.217-1.248
moderate	1.199	0.005	1.194	1.204					1.194-1.204
CWC									
very slight	0.037	0.001	0.037	0.038	0.039	0.0004	0.038	0.039	0.037-0.039
slight	0.032	0.001	0.032	0.033	0.035	0.0004	0.035	0.036	0.032-0.036
moderate	0.027	0.001	0.026	0.028					0.026-0.028

Note: *in bold are the ranges of pixel variation without overlapping.

L. dispar. The minimal overlap between these levels further emphasizes their effectiveness in accurately capturing and differentiating defoliation levels. Furthermore, the CWC biophysical index exhibits distinct ranges of pixel value variation in the two years, indicating a higher level of stability of this index for assessing the defoliation caused by *L. dispar*. Additionally, graphical representations were created to illustrate the ranges of pixel value variation for each level of defoliation across the different vegetation indices (Figure 7).

These graphical representations provide a visual understanding of how the pixel



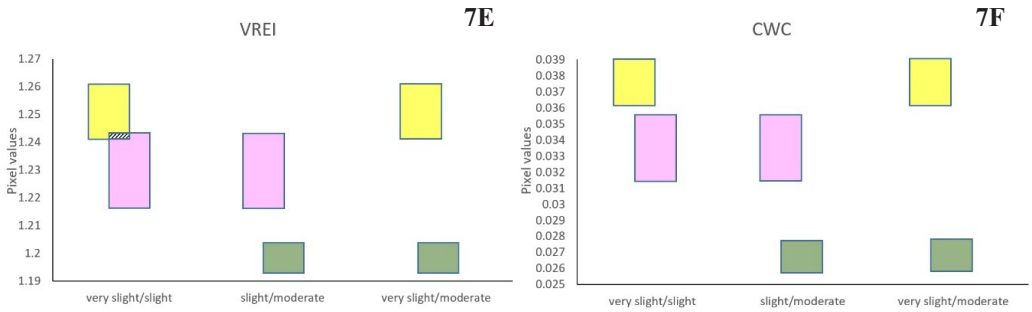
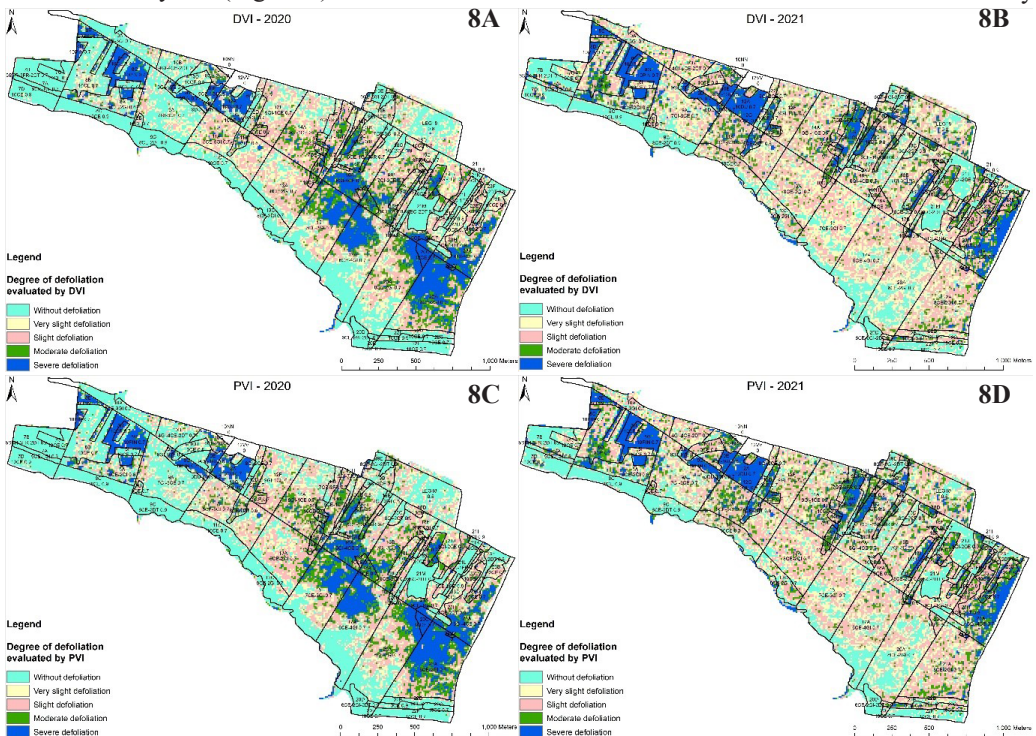


Figure 7 The ranges of variation of the pixel values for derived indices, by levels of defoliation, for the sampled area of the Ciuturica forest (yellow areas represent the ranges of pixel values for very slight defoliation, pink areas – the slight defoliation, green areas - moderate defoliation and hatched areas indicate the ranges for the overlapping of the defoliation levels) – NDVI (A), DVI (B), PVI (C), NDRE (D), VREI (E), CWC (F).

values vary within each defoliation level. The thematic maps, generated using the statistically validated indices (DVI, PVI, VREI and CWC) derived from Sentinel 2 images and classified into ranges of pixel value variation specific to each level of defoliation, provided valuable information for calculating the defoliation areas for both years (Figure 8).

The comparative analysis of surfaces categorized by levels of defoliation, derived from thematic maps based on pixel variation intervals for the CWC biophysical index and vegetation indices (DVI, PVI, VREI), along with those calculated from field-based observations, revealed certain differences in the estimated areas. These differences were observed not only



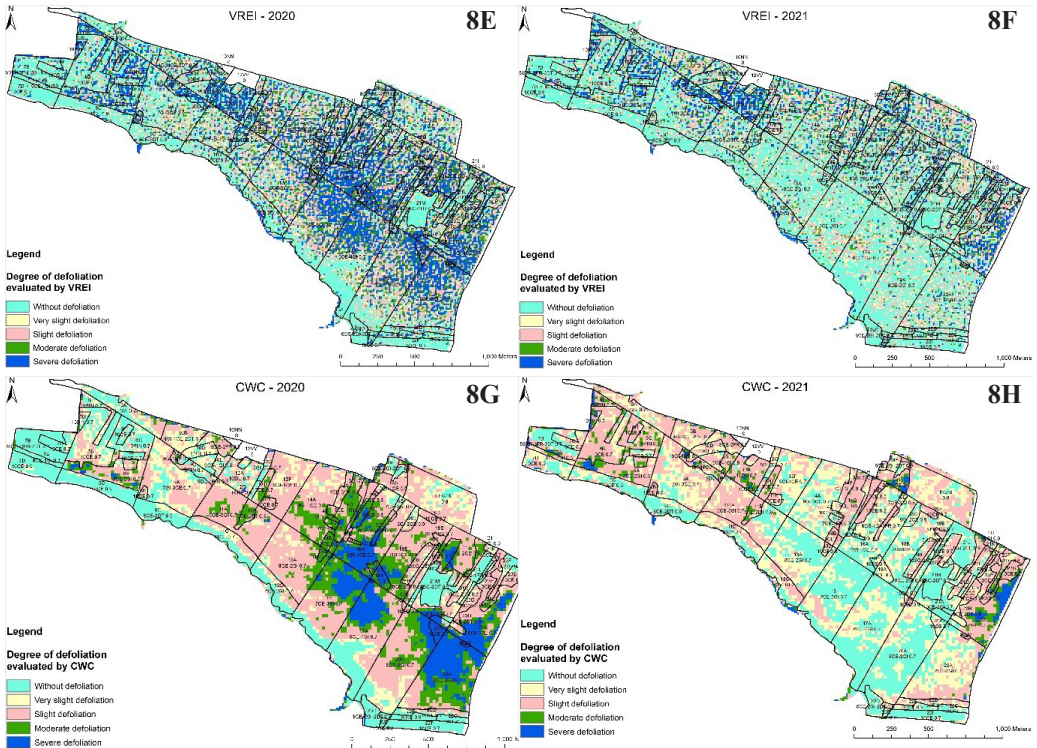


Figure 8 Thematic maps obtained based on field defoliation assessment and based on Sentinel 2 images specified indices assessments (DVI, PVI, VREI, CWC) for the years 2020 (DVI – A), PVI – C), VREI – E), CWC – G) and 2021 (DVI – B), PVI – D), VREI – F), CWC – H).

between the field-based estimations and index-based calculations but also among the individual indices themselves (Figure 9).

The negative differences observed in the estimated areas on thematic maps compared

to ground-based assessments, specifically for areas without defoliation, can be partly attributed to the subjectivity of the field assessment teams, which sometimes may tend to classify non-defoliated trees as very

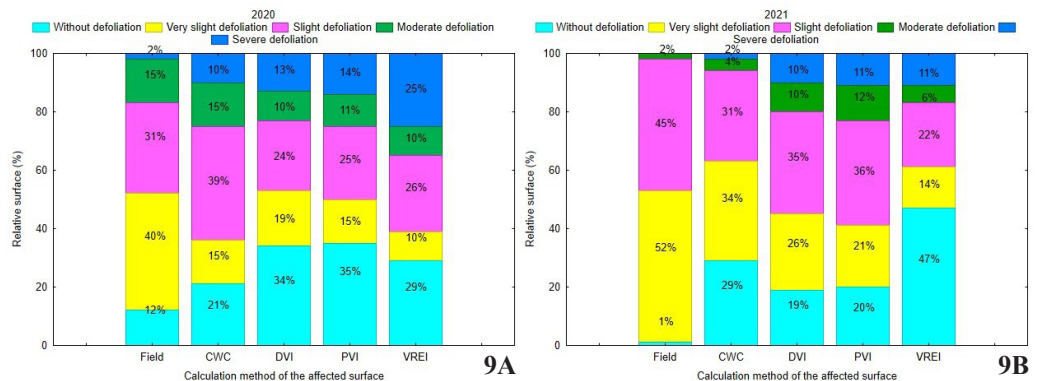


Figure 9 The comparative assessment of the surfaces affected by defoliation (%), by level of the affected defoliation, based on field observations and indices derived based on Sentinel 2 satellite images, for 2020 (A) and 2021 (B).

slight defoliated ones. Moreover, additional differences observed in the areas estimated on the thematic maps derived from indices compared to those calculated based on ground data can be attributed to systematic errors of defoliation underestimation by the operators. These errors may arise due to the limitations of visual field assessment, where the operators might not always have a clear view of the upper part of the crown, which is often the most affected by defoliation. In contrast, use of high-resolution satellite images (i.e., Sentinel 2 satellite images) provide better visibility, capturing the extent of defoliation more accurately.

Discussion

The assessment of damage caused by *Lymantria dispar* using satellite images with various temporal and spatial resolutions has been widely investigated in various regions worldwide (Beurs & Townsend 2008, Pasquarella et al. 2018, Choi et al. 2021). These studies have emphasized the effectiveness of various vegetation indices, such as NDVI (Normalized Difference Vegetation Index), EVI (Enhanced Vegetation Index), NDMI (Normalized Difference Moisture Index), and the Greenness index derived from the Tasseled Cap transformation, in detecting and quantifying defoliation levels, identifying affected areas, and monitoring the spatial patterns and severity of damage. The NDVI, widely recognized as the predominant remote sensing index for assessing vegetation health (Huang et al. 2021), was employed in a study conducted by Spruce et al. (2011). Their research used Moderate Resolution Imaging Spectroradiometer (MODIS) satellite products from 2000-2006 to generate defoliation maps caused by *L. dispar* within a specific area situated in the mid-Appalachian highland region of the United States. The findings of the study unequivocally showcased the efficacy of employing regional products derived from processing MODIS NDVI time series to accurately indicate the extent of defoliation

caused by *L. dispar*. In a comprehensive case study by Pasquarella et al. (2018), focused on gypsy moth defoliation in southern New England between 2015 and 2017, the use of the Tasseled Cap Greenness index and Landsat 7 and 8 satellite time series was proposed. The study's findings highlighted the significance of leveraging remote sensing data to comprehensively understand and monitor the impact of gypsy moth defoliation. In a recent study conducted by Pasquarella et al. (2021), it was found that Landsat satellite time series, coupled with the Tasseled Cap Greenness, Simple Ratio, and Enhanced Vegetation Index (EVI), emerged as the most valuable remote sensing indices for predicting gypsy moth-induced defoliation in Southern New England during the period of 2016-2018.

In a noteworthy study conducted by Choi et al. (2021), it was conclusively demonstrated that the use of a canopy-related index (NDMI), derived from Landsat satellite images, enabled the successful detection of areas impacted by gypsy moth defoliation, laying the foundation for conducting outbreak risk analysis by effectively identifying regions susceptible to gypsy moth infestation based on their defoliation patterns.

In a recent study, Hawryło et al. (2018) employed Sentinel 2 data in conjunction with various machine learning algorithms to evaluate defoliation levels in Scot pine stands located in western Poland. The study's findings unveiled that vegetation indices derived from Sentinel 2 images, specifically the Green Normalized Difference Vegetation Index and MERIS Terrestrial Chlorophyll Index, proved to be the most effective for accurately assessing the extent of defoliation.

The present study aimed to explore the potential of satellite remote sensing methods for monitoring, assessing, and classifying tree damage caused by the *L. dispar* defoliator. The characteristics of the damages caused by *L. dispar* to oak tree species do not vary significantly across different phytoclimatic

regions. Therefore, the findings of this research can be replicated in other regions in order to assess the defoliation caused by this insect. To the best of our knowledge, this is the first study conducted in Romania that uses high spatial resolution satellite images, such as Sentinel-2, for monitoring and assessing the defoliation caused by *L. dispar*.

In this regard, by analyzing the pixel values of specific indices derived from Sentinel 2 satellite images and comparing them with defoliation values estimated using field methodology, a significant correlation was observed. The correlation coefficients between the pixel values of the indices and the estimated defoliation values were found to be between 0.53 (NDVI) and 0.74 (CWC) for the year 2020, and between 0.48 (NDRE) and 0.62 (CWC) for the year 2021. These correlation coefficients indicate a close relationship between the satellite-derived indices and the field-based defoliation assessments.

When visually comparing the two types of thematic maps, based on ground observations and specific indices derived from satellite images, it is observed that among all the statistically significant indices, the biophysical index CWC offered the best results. For the year 2020, the spatial distribution of defoliation levels based on the CWC index closely resembled the results obtained from ground observations. In the year 2021, a similar trend was observed in the spatial distribution of defoliation levels based on the CWC index, although to a lesser extent compared to the previous year. These differences in the trend observed between the two years, as provided by the CWC index, can be attributed to several factors, including the subjectivity of field team assessment of the defoliation. It is not uncommon for field operators to slightly overestimate the very slight intensity defoliation. Furthermore, the comparative analysis revealed that the CWC biophysical index demonstrates the highest capability in capturing both areas without defoliation and

those affected by different levels of defoliation caused by *L. dispar*.

However, the thematic maps obtained based on the vegetation indices (DVI, PVI, and VREI), which have been proven to be statistically significant, do not show the same level of accuracy in capturing the distribution of defoliation levels across the Ciuturica forest. Furthermore, the research carried out in this study serve as a foundation for future investigations involving damage assessment of various harmful biotic agents using remote sensing specific techniques. Such endeavors significantly contribute to advancing the application of these techniques within the field of monitoring and assessing the phytosanitary condition of forests. In this regard, future research for other defoliating insects, such as *Tortrix viridana*, that cause defoliation during early spring when tree foliage is not fully developed, or the Geometridae species that initiate defoliation at the base of the crown, are necessary in order to confirm the accuracy and applicability of remote sensing indices in assessing defoliation levels.

Conclusions

The research study has highlighted that the CWC index is consider to be highly suitable for assessing defoliation caused by *Lymantria dispar*. Furthermore, it recorded a strong intensity correlation in relation to the intensities of defoliation assessed by field operators, and the ranges of pixel value variation, according to levels of defoliation, did not overlap. The thematic maps generated using the pixel variation intervals for the CWC biophysical index and the vegetation indices DVI, PVI, and VREI allowed for the calculation of defoliation-affected areas classified by levels of defoliation. A comparative analysis was then conducted by comparing these areas with the surfaces obtained from the thematic maps based on the field observations. The results of the comparative analysis revealed certain trends. Both the CWC biophysical

index and the vegetation indices (DVI, PVI, VREI) tended to overestimate the forest areas that were not affected by defoliation and to slightly underestimate the areas affected by very slight and slight defoliation. The results of the study highlight that remote sensing derived indices based on Sentinel 2 images used for monitoring and assessing the impacts of the *L. dispar*, which causes tree defoliation, can complement field-based surveillance and control processes. Furthermore, these remote sensing techniques are particularly valuable for assessing large forested areas or inaccessible regions where ground-based observations may be challenging.

Acknowledgement

This research was made possible through the funding provided by the Romanian Ministry of Research, Innovation and Digitalization, FORCLIMSOC Nucleu Programme (Contract 12N/2023), project PN 23090102 and project „Creșterea capacității și performanței instituționale a INCDS „Marin Drăcea” în activitatea de CDI - CresPerfInst” (Contract 34PFE/30.12.2021).

Declaration of the authors

The authors declare there is no conflict of interest regarding the publishing of the paper, which does not include any form of plagiarism.

References

Ali A.M., Darvishzadeh R., Skidmore A., Gara T.W., O'Connor B., Roesli C., Heurich M., Paganini M., 2020. Comparing methods for mapping canopy chlorophyll content in a mixed mountain forest using Sentinel-2 data. *International Journal of Applied Earth Observation and Geoinformation*, 87:102037. <https://doi.org/10.1016/j.jag.2019.102037>

Arhrib Y.J., Francini S., D'Amico G., Castedo-Dorado F., Garnica-López J., Álvarez-Taboada M.F. 2023. Web application based on Sentinel-2 satellite imagery for water stress detection and monitoring in poplar plantations. In: Benítez-Andrades J.A., García-Llamas P., Taboada Á., Estévez-Mauriz L., Baelo R. (eds) *Global Challenges for a Sustainable Society. EURECA-PRO 2022*. Springer Proceedings in Earth and Environmental Sciences. Springer, Cham. https://doi.org/10.1007/978-3-031-25840-4_38

Badea O., 2008. Manual privind metodologia de

supraveghere pe termen lung a stării ecosistemelor forestiere aflate sub acțiunea poluării atmosferice și modificărilor climatice. Ed. Silvică, ISBN 978-973-88379-5-9, 98 p.

Badea O., Silaghi D., Taut I., Neagu S., Leca S., 2013. Forest monitoring – assessment, analysis and warning system for forest ecosystem status. *Notulae Botanicae Horti Agrobotanici Cluj – Napoca*, 41(2):613-625. <https://doi.org/10.15835/nbha4129304>

Barnes E.M., Clarke T.R., Richards S.E., Colaizzi P.D., Haberland J., Kostrzewski M., Waller P., Choi C., Riley E., Thompson T., Lascano R.J., Li H., Moran M.S., 2000. Coincident detection of crop water stress, nitrogen status and canopy density using ground based multispectral data. In *Proceedings of the 5th International Conference on Precision Agriculture*. Bloomington, Minnesota, USA, 16-19 July, 2000, 1619:1-15.

Beaubien J., Jobin L., 1974. ERTS-1 imagery for broad mapping of forest damage and cover types of Anticosti Island. *Canadian Surveyor*, 28(2):164-166.

Berryman A.A., 1986. *Forest insects: principles and practice of population management*. Plenum Press, New York and London, 279 p. eBook ISBN 9781468450804, Published: 06 December 2012. <https://doi.org/10.1007/978-1-4684-5080-4>

Beurs K.M. de, Townsend P.A., 2008. Estimating the effect of gypsy moth defoliation using MODIS. *Remote Sensing of Environment*, 112(10):3983-3990. <https://doi.org/10.1016/j.rse.2008.07.008>

Cernicharo J., Verger A., Camacho F., 2013. Empirical and physical estimation of canopy water content from CHRIS/PROBA Data. *Remote Sensing*, 5(10):5265-5284. <https://doi.org/10.3390/rs5105265>

Chávez R.O., Rocco R., Gutiérrez Á.G., Dörner M., Estay S.A., 2019. A self-calibrated non-parametric time series analysis approach for assessing insect defoliation of broad-leaved deciduous *Nothofagus pumilio* forests. *Remote Sensing*, 11(2):204. <https://doi.org/10.3390/rs11020204>

Choi W.I., Kim E.S., Yun S.J., Lim J.H., Kim Y.E., 2021. Quantification of one-year gypsy moth defoliation extent in Wonju, Korea, using landsat satellite images. *Forests*, 12(5):545. <https://doi.org/10.3390/f12050545>

Ciesla W., Billings R., Compton J., Frament W., Mech R., Roberts M., 2008. Aerial signatures of forest damage in the Eastern United States. The Forest Health Technology Enterprise Team (FHTET), USA, 121 p.

Clarke T.R., Moran M.S., Barnes E.M., Pinter P.J., Qi J., 2001. Planar domain indices: A method for measuring a quality of a single component in two-component pixels. In *IGARSS 2001. Scanning the Present and Resolving the Future*. Proceedings. IEEE 2001 International Geoscience and Remote Sensing Symposium (Cat. No. 01CH37217), Sydney, NSW, Australia, 3, pp. 1279-1281. <https://doi.org/10.1109/IGARSS.2001.976818>

Crocker E., Gurung K., Calvert J., Nelson C.D., Yang J., 2023. Integrating GIS, remote sensing, and citizen science to map oak decline risk across the Daniel Boone National Forest. *Remote Sensing*, 15(9):2250. <https://doi.org/10.3390/rs15092250>

Curran P.J., 1989. Remote sensing of foliar chemistry.

- Remote Sens. Environ., 30(3):271–278. [https://doi.org/10.1016/0034-4257\(89\)90069-2](https://doi.org/10.1016/0034-4257(89)90069-2)
- El Ahmadi S., Ramzi H., Aafi A., Jmii N.E., Aadel T., 2023. Assessment of cork oak decline using digital multispectral imagery in relation with in situ crown condition. *Open Journal of Forestry*, 13(1):145-160. <https://doi.org/10.4236/ojf.2023.131010>
- Fleming R., Volney W., 1995. Effects of climate change on insect defoliator population processes in Canada's boreal forest: Some plausible scenarios. *Water, Air, Soil Pollution* 82:445-454. <https://doi.org/10.1007/BF01182854>
- Fraser R., Latifovic R., 2005. Mapping insect-induced tree defoliation and mortality using coarse spatial resolution satellite imagery. *Int J of Remote Sens* 26(1):193-200. <https://doi.org/10.1080/01431160410001716923>
- Gupta S.K., Pandey A.C., 2021. Spectral aspects for monitoring forest health in extreme season using multispectral imagery. *The Egyptian Journal of Remote Sensing and Space Science*, 24(3): 579-586. <https://doi.org/10.1016/j.ejrs.2021.07.001>
- Hall R.J., Castilla G., White J.C., Cooke B.J., Skakun R.S., 2016. Remote sensing of forest pest damage: a review and lessons learned from a Canadian perspective. *The Canadian Entomologist*, 148, Supplement S1: Forest Entomology in Canada: Celebrating a Century of Science Excellence, August 2016:S296 - S356. <https://doi.org/10.4039/tce.2016.11>
- Hawryło P., Bednarz B., Wężyk P., Szostak M., 2018. Estimating defoliation of Scots pine stands using machine learning methods and vegetation indices of Sentinel-2. *European Journal of Remote Sensing*, 51(1): 194-204. <https://doi.org/10.1080/22797254.2017.1417745>
- Huang S., Tang L., Hupy J.P., Wang Y., Shao G., 2021. A commentary review on the use of normalized difference vegetation index (NDVI) in the era of popular remote sensing. *Journal of Forestry Research*, 32(1):1-6. <https://doi.org/10.1007/s11676-020-01155-1>
- Hunt Jr.E.R., Daughtry C.S.T., Eitel J.U., Long D.S., 2011. Remote sensing leaf chlorophyll content using a visible band index. *Agronomy Journal*, 103(4):1090-1099. <https://doi.org/10.2134/agnonj2010.0395>
- Innes J., 1993. *Forest health: its assessment and status*. Cab International, Wallingford, UK. ISBN: 9780851987934, 677 p.
- Marceau D., Hay G., 1999. Remote sensing contributions to the scale issue. *Can J Remote Sens* 25(4):357-366. <https://doi.org/10.1080/07038992.1999.10874735>
- Marx A., Kleinschmit B., 2017. Sensitivity analysis of RapidEye spectral bands and derived vegetation indices for insect defoliation detection in pure Scots pine stands. *iForest-Biogeoeciences and Forestry*, 10(4):659-668. <https://doi.org/10.3832/ifer1727-010>
- Norma 6/2000, OG 454/2003. Norma tehnică pentru protecția pădurilor din 14.07.2003. MAPAM. Monitorul Oficial, Partea I nr. 564 din 06 august 2003.
- Pasquarella V.J., Elkinton J.S., Bradley B.A., 2018. Extensive gypsy moth defoliation in Southern New England characterized using Landsat satellite observations. *Biological Invasions*, 20:3047-3053. <https://doi.org/10.1007/s10530-018-1778-0>
- Pasquarella V.J., Mickley J.G., Barker Plotkin A., MacLean R.G., Anderson R.M., Brown L.M., Wagner D.L., Singer M.S., Bagchi R., 2021. Predicting defoliator abundance and defoliation measurements using Landsat-based condition scores. *Remote Sensing in Ecology and Conservation*, 7(4):592-609. <https://doi.org/10.1002/rse2.211>
- Richardson A.J., Wiegand C.L., 1977. Distinguishing vegetation from soil background information. *Photogrammetric Engineering and Remote Sensing*, 43(12):1541-1552.
- Rouse J.W., Haas R.H., Schell J.A., Deering D.W., 1974. Monitoring vegetation systems in the great plains with ERTS. Third ERTS-1 Symposium NASA, NASA SP-351, Washington DC, 309-317.
- Rullan-Silva C.D., Olthoff A.E., Delgado de la Mata J.A., Pajares-Alonso J.A., 2013. Remote monitoring of forest insect defoliation. *A review. Forest Systems*, 22(3):377-391. <https://doi.org/10.5424/fs/2013223-04417>
- Sturtevant B.R., Cooke B.J., James P.M., 2023. Of clockwork and catastrophes: Advances in spatiotemporal dynamics of forest Lepidoptera. *Current Opinion in Insect Science*, 101005. <https://doi.org/10.1016/j.cois.2023.101005>
- Spruce J.P., Sader S., Ryan R.E., Smoot J., Kuper P., Ross K., Prados D., Russell J., Gasser G., McKellip R., Hargrove W., 2011. Assessment of MODIS NDMI time series data products for detecting forest defoliation by gypsy moth outbreaks. *Remote Sensing of Environment*, 115(2):427-437. <https://doi.org/10.1016/j.rse.2010.09.013>
- Tucker C.J., 1979. Red and photographic infrared linear combinations for monitoring vegetation. *Remote Sensing of Environment*, 8(2):127-150. [https://doi.org/10.1016/0034-4257\(79\)90013-0](https://doi.org/10.1016/0034-4257(79)90013-0)
- Volke M.L., Abarca-del-Rio R., 2020. Comparison of machine learning classification algorithms for land cover change in a coastal area affected by the 2010 Earthquake and Tsunami in Chile. *Natural Hazards and Earth System Sciences Discussions*, 1-14 [preprint]. <https://doi.org/10.5194/nhess-2020-41>
- Vogelmann J.E., Rock B.N., Moss D.M., 1993. Red edge spectral measurements from sugar maple leaves. *International Journal of Remote Sensing*, 14(8):1563–1575. <https://doi.org/10.1080/01431169308953986>
- Vorovencii I., 2015. *Teledetectie satelitară*. Ed. MatrixRom, București, ISBN: 978-606-25-0142-6, 600 p.
- Weiss M., Baret F., Jay S., 2020. S2ToolBox Level 2 products LAI, FAPAR, FCOVER. Doctoral dissertation, EMMAH-CAPTE, INRA Avignon.
- Wulder M., Franklin S., 2006. Understanding forest disturbance and spatial pattern: Remote sensing and GIS approaches. eBook ISBN 9780429114434, Taylor & Francis Group, FL, USA. 246 p. <https://doi.org/10.1201/9781420005189>
- Xue J., Su B., 2017. Significant remote sensing vegetation indices: A review of developments and applications. *Journal of Sensors*, 2017: 1353691. <https://doi.org/10.1155/2017/1353691>